



**PROBA 2 - LYRA**  
**Calibration PTB-Bessy II**

Doc. Reference  
Date:  
Issue:  
Page: 1 of 18

## **Calibration Report NI beamline (40-240nm)**

### **PROBA-2 / LYRA**

**July 2005**

Doc. RP-ROB-LYR-0132-NI-July2005

issue Version 1.2  
01 September 2005

Prepared by : A. BEN MOUSSA (ROB)  
Verified by : A. THEISSEN  
Released by : J-F. HOCHEDÉZ



**PROBA 2 - LYRA**  
**Calibration PTB-Bessy II**

Doc. Reference  
Date:  
Issue:  
Page: 2 of 18

## Distribution List

Recipients	Affiliation	Nr. of Copies
LYRA team	CSL, IMO, PMOD, MPS, IEMN, ROB	Email copy
H. Schroeven-Deceuninck	ESA/PRODEX	“

## Document Change Record

Issue	Date	Comments
1.1	25 August 2005	initial issue
1.2	1 Sept 2005	Updated (corrected data homogeneity channel 2-1) +Annexe



## Table of Contents

<b>1</b>	<b>Execution Plan for LYRA</b>	<b>4</b>
<b>2</b>	<b>RESULTS</b>	<b>5</b>
<b>2.1</b>	<b>Flux Linearity at 121.6 and 200nm</b>	<b>5</b>
<b>2.2</b>	<b>Stability (Drift) at 121.6 and 210nm</b>	<b>7</b>
<b>2.3</b>	<b>Spectral responsivity (110-240nm)</b>	<b>9</b>
2.3.1	Lyman- $\alpha$ channels (MSM12-21 and AXUV#56)	10
2.3.2	Herzberg channels (PIN 10-11-12)	11
<b>3</b>	<b>Homogeneity</b>	<b>13</b>
<b>3.1</b>	<b>HEAD 1: Ch 1-1; 1-2; 1-3</b>	<b>13</b>
<b>3.2</b>	<b>HEAD 2: Ch 2-1; 2-2; 2-3</b>	<b>13</b>
<b>3.3</b>	<b>HEAD 3: Ch 3-1; 3-2; 3-3</b>	<b>14</b>
<b>4</b>	<b>CONCLUSION</b>	<b>14</b>
<b>5</b>	<b>ANNEXE</b>	<b>15</b>

## Reference documents

[RD1] : LYRA\_NI\_Instrument\_Calibration\_Plan-V1.3.doc (ROB)

[RD2] : LYRA\_Assembly\_270705.xls (PMOD)



## Scope

The purpose of this report is to summarize/analyse results from the NI calibration campaign at PTB-Bessy II (July 2005).

## 1 Execution Plan for LYRA

The PTB campaign plan was executed as following:

Activities number	Activities name	Remark
1	Linearity vs Flux at $\lambda_{1,2}$	See RD1
2	Stability vs Time at $\lambda_{1,2}$	“
3	Spectral responsivity	“
4	Homogeneity	“
5*	Check for holes in Zr and Al channels	“

\* Scanning over the Zr and Al channels, no significant signals were measured, i.e no holes.



## 2 RESULTS

### 2.1 Flux Linearity at 121.6 and 200nm

To avoid saturation of the electronics, the linearity was investigated using different aperture stops or by varying the exit slit of the respective monochromator.

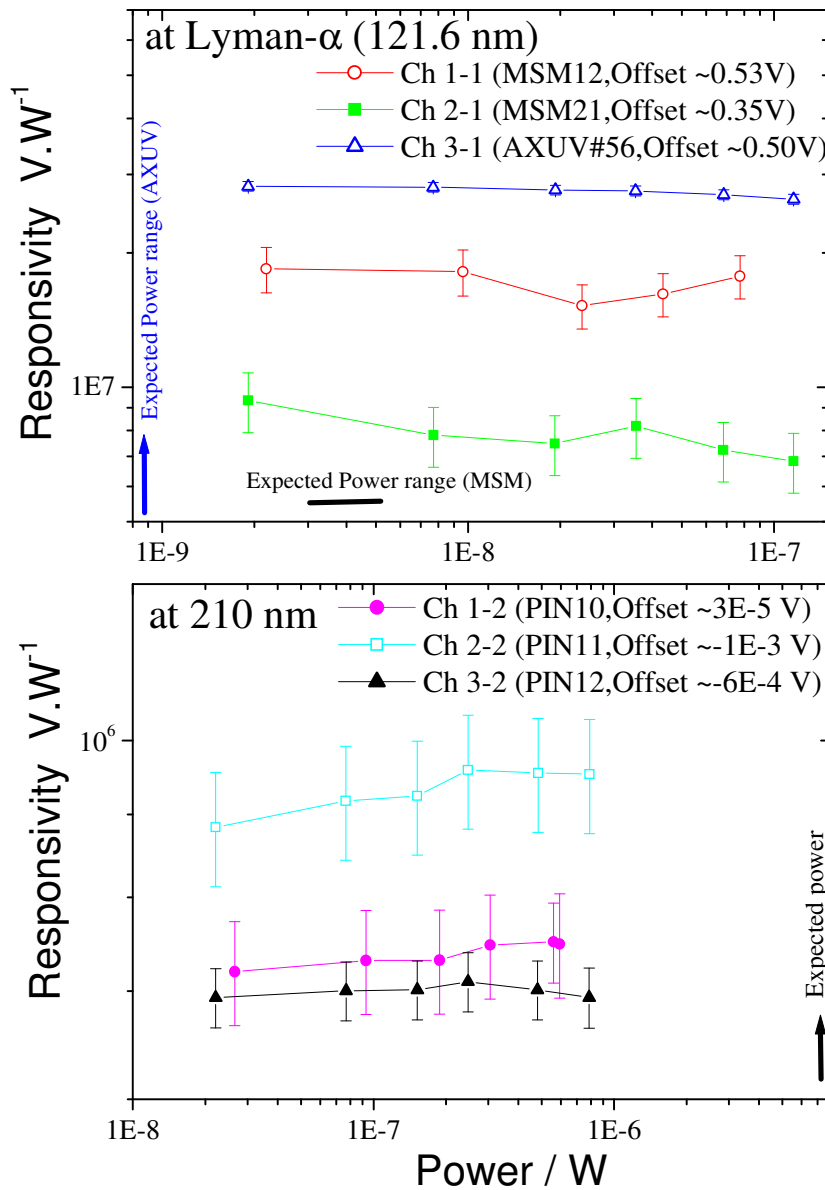


**Figure 1.** Flux linearity of Ly- $\alpha$  and Herzberg channels (Response vs. incident power) at 121.6 and 210 nm. The lines are guides for the eye.



**PROBA 2 - LYRA**  
**Calibration PTB-Bessy II**

Doc. Reference  
Date:  
Issue:  
Page: 6 of 18

The responsivity of the Ly- $\alpha$  channels (1-1; 2-1) decreases with increasing incident light power up to ~ 20-30 nW after which the responsivity starts to increase and then to decrease again for MSM21. For the AXUV channel, the responsivity remains almost constant indicating a linear response, then slightly decreases indicating a sublinear response (using a power law:  $I = aP^b$ ;  $R \propto P^{b-1}$ ;  $b = 1$  for linear response). The responsivity of the Herzberg channels (1-2; 2-2 and 3-2) at 210 nm increases with increasing incident light power roughly until 200-300nW (superlinear) then remains almost constant for channels 1-2 and 2-2 but decrease for the channel 3-2 (sublinear).

According to the previous calibration campaign, MSM were sublinear and PIN superlinear vs the whole power range of the photon flux. It should be noticed that the temperature inside the LYRA was around 60°C. The expected radiant power in orbit for the different LYRA channels are shown in Figure 1 and Table 1.

**Table 1** : Expected radiant power for solar Min,  $\Phi_{min}$ [W], and for solar Max,  $\Phi_{max}$  [W], through the aperture (3mm  $\varnothing$ ) for the 5 different channels.

			$\Phi_{min}$	$\Phi_{max}$
<b>HEAD 1 or 2</b>	<b>Channel 1</b>	<b>Ly-<math>\alpha</math> (XN122)</b>	3,7 nW	5 nW
	<b>Channel 2</b>	<b>Herzberg</b>	7,4 $\mu$ W	7,4 $\mu$ W
	<b>Channel 3</b>	<b>Aluminium</b>	4,4 nW	131 nW
	<b>Channel 4</b>	<b>Zirconium</b>	5,6 nW	146,5 nW
<b>HEAD 3</b>	<b>Channel 1</b>	<b>Ly-<math>\alpha</math> (XN122+N)</b>	0,647nW	0,888nW



## 2.2 Stability (Drift) at 121.6 and 210nm

The stability of the output signal under irradiation over prolonged periods is a mission goal for a solar instrument like LYRA. The signal stability was measured at 60°C at **121.6nm** (corresponding to the H I Lyman- $\alpha$  wavelength) and **210nm** wavelength. The shutter was opened and closed approximately every 60s (short period) and every 580s (long period). The data are corrected for the small decline (1%) of the current of the synchrotron storage ring during the time period of each measurement. Voltage units were changed to current units (A) using the appropriate gain resistor [see RD2].

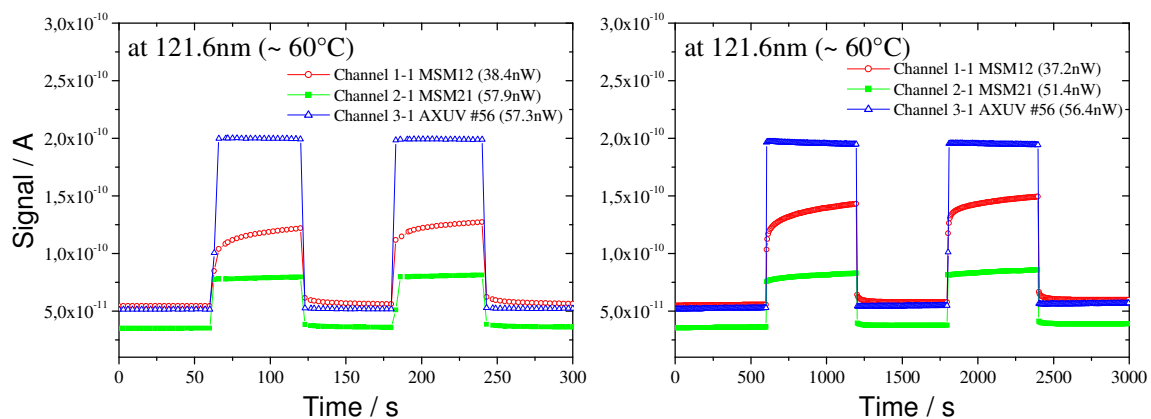


**Figure 2.** Absolute signal in ampere of Ly- $\alpha$  channels as a function of time at 121.6 nm (left) for a short period and (right) for a long period. The lines are guides for the eye.

As seen in the figures, channel 1-1 (MSM12) is not stable under irradiation (the signal increases with time) and shows a dark current drift. When the shutter is closed, the dark current decreases slowly with a progressive return to an equilibrium condition. It shows a decay from 55 to 59 pA at 121.6 nm. The initial dark current seems to be dependent on duration and on the flux of previous exposures, consistent with the rather long time constants observed. Channel 2-1 (MSM21) looks more stable. The signal increases by +2% for a short time exposure (50s) and by +6-7% after 550s. This remains to be explained and may be a concern for LYRA operation. The dark current is lower at around 35pA. Channel 3-1 (AXUV) shows a good stability on a short temporal range with a dark current of around 50-55pA. For a longer exposure time, the signal decreases progressively with a signal drift of less than 0.7%.

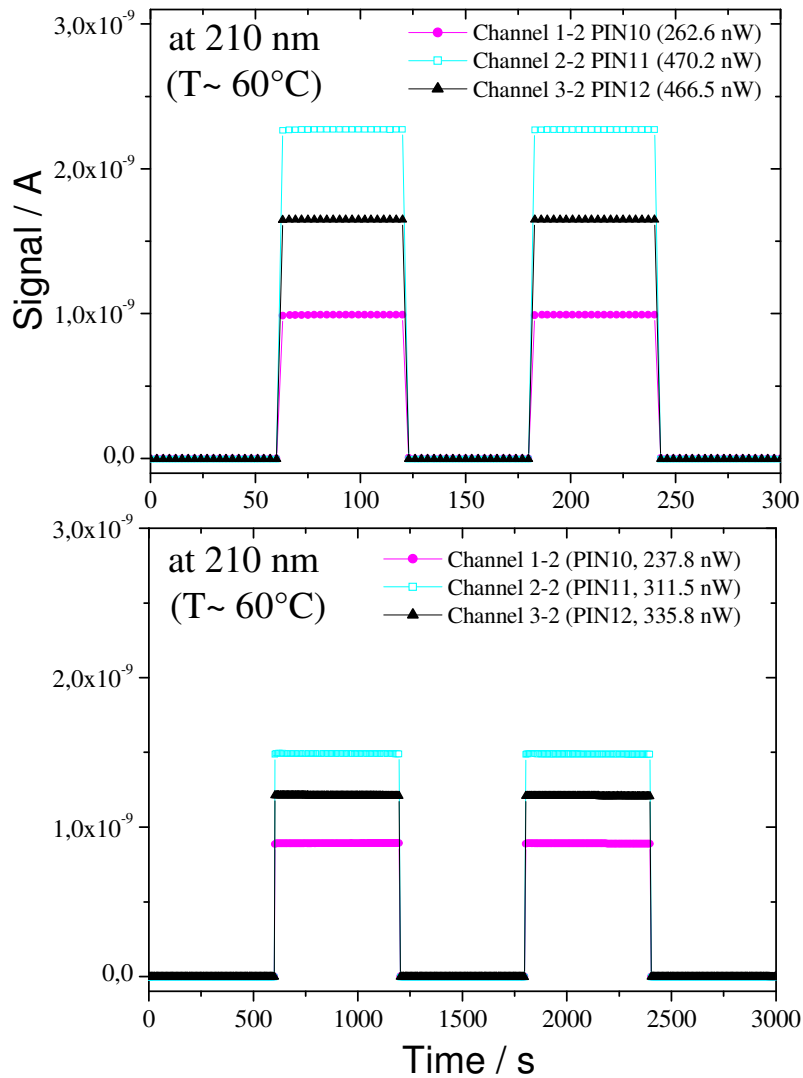


**Figure 3.** Absolute signal in ampere of Herzberg channels as a function of time at 210 nm (left) for a short period and (right) for a long period. The lines are guides for the eye.

Herzberg channels (2-1; 2-2; 3-2) show a good stability over a wide temporal range with a negligibly small background detrapping current of approximately  $1 \times 10^{-13}$  A. This variation is insignificant in absolute terms. The fact that the pin diode operates in unbiased mode (i.e. it does not require an external voltage) implies a very low dark current. It can be observed that the





diamond PINs respond fast to the signal change with an exact return to its initial dark-signal values after irradiation (note that we have a negative offset of  $-3 \times 10^{-12}$  A for channel 2-2 and 3-2).

The responsivity of the detectors (i.e. solar-blindness) will be monitored by on-board light sources (UV-LEDs emitting at 375 nm) to distinguish the detector's drift from inevitable degradations of the filters. A test was performed at Ly- $\alpha$  (see Fig.4) to check if the MSM signal can be improved (i.e be made more stable) by switching "ON" the LEDs (when the localized empty states are filled, the signal remains stable).

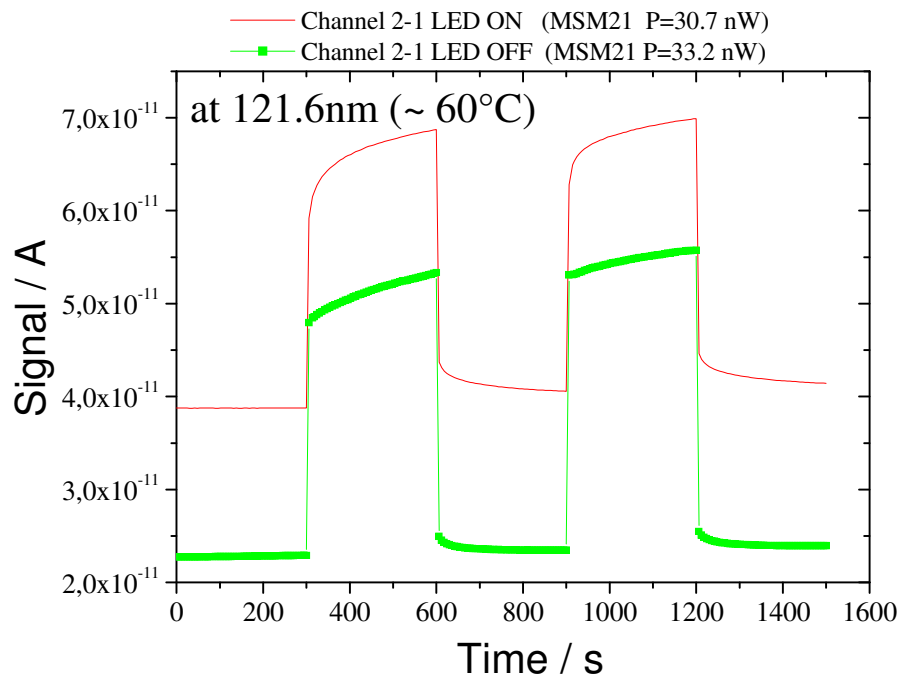


**Figure 4.** Absolute signal in ampere of channel 2-1 (MSM21) as a function of time at 121.6 nm with LEDs On and OFF.

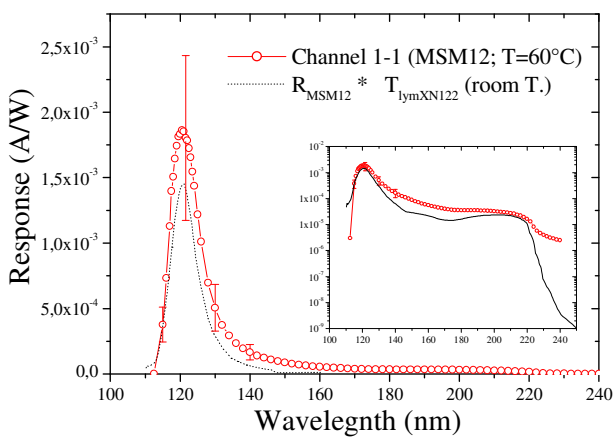
Figure 4 shows that the performance of the detector does not change with the LEDs "ON". The offset increases from  $2,4E-11$  to  $4E-11$  A.

### 2.3 Spectral responsivity (110-240nm)

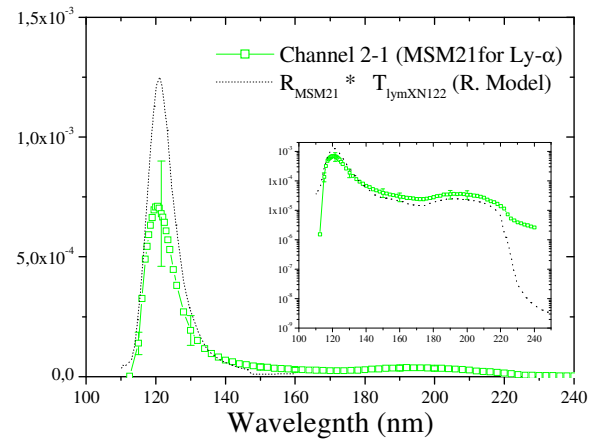
The responsivity for LYRA channels were measured in the center position (except for 2-1) at regular intervals and in finest steps close to Ly- $\alpha$  and Herzberg range. The calibration positions should be taken into account (especially for MSM channels, see homogeneity graph in Annexe). Voltage units were changed to current units (A) using the appropriate gain resistor [see RD2].



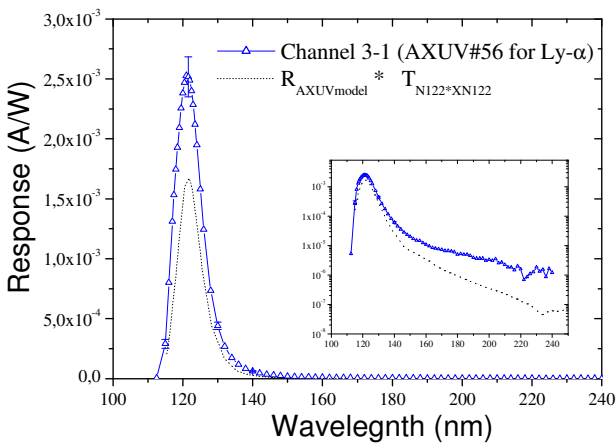
### 2.3.1 Lyman- $\alpha$ channels (MSM12-21 and AXUV#56)



Offset: 0.5721V; PosH=4,6; PosV=87,8



Offset: 0.3524V; PosH=4.45; PosV=149.3



Offset: 0.5704V PosH=3.95 PosV=210.2

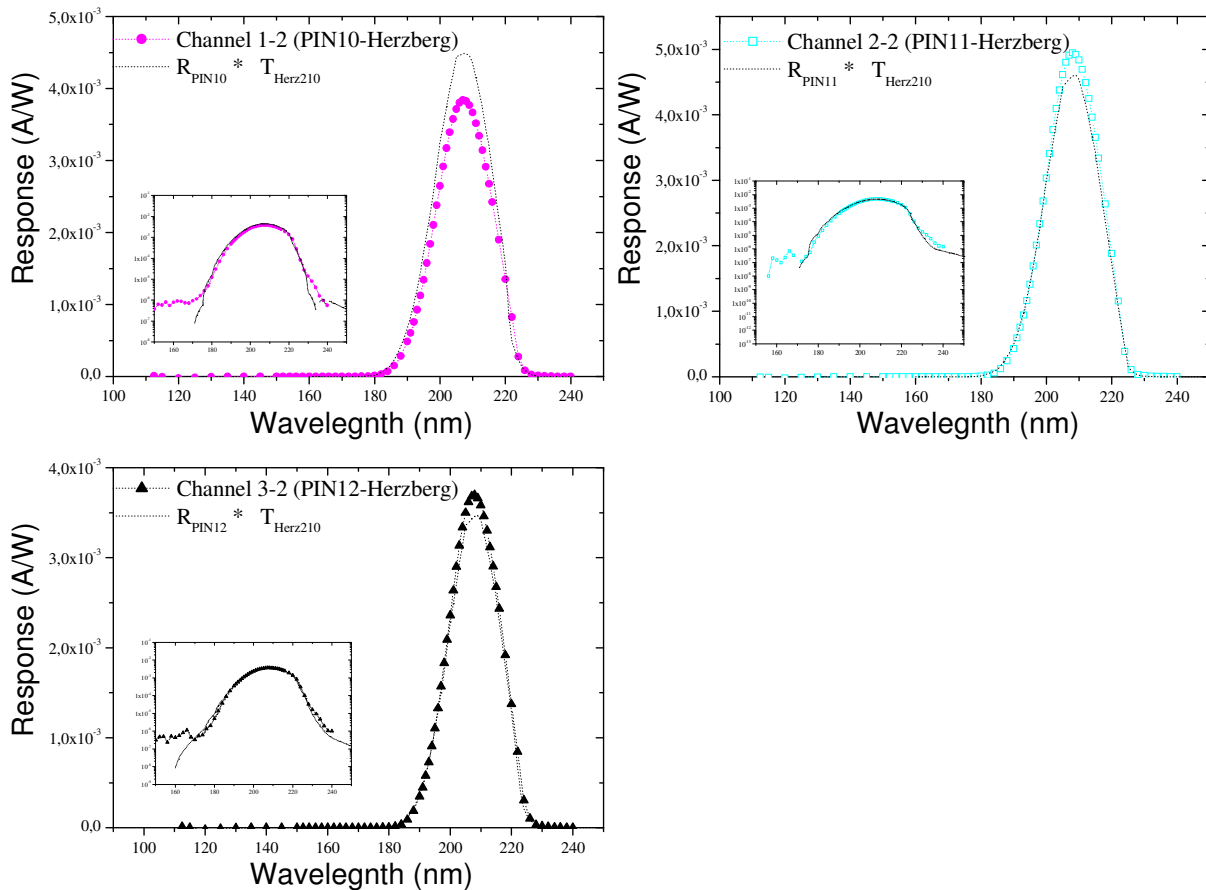
**Figure 5.** Absolute spectral responsivity (in A/W) of channel 1-1, 2-1 and 3-1 between 110nm and 240 nm. For comparison, the dotted line represents the model used in the LYRA radiometric model (detector R x Filter T).

Fig. 5 shows that some channels were either over or underestimated by our radiometric model. Note that the uncertainties, especially for the MSM channels, are very high. One possible explanation is a temperature effect on filters and detectors ( $T=60^{\circ}\text{C}$ ).



### 2.3.2 Herzberg channels (PIN 10-11-12)

We did not plot the estimated error bars to the data since they are negligible.



**Figure 6.** Absolute spectral responsivity (in A/W) of channel 1-2, 2-2 and 3-2 between 110nm and 240 nm. For comparison, the dotted line represents the model used in the LYRA radiometric model (detector R x Filter T).

Table 2 summarizes the derived results using the TIME-SEE solar spectrums. More information can be found in the updated LYRA radiometric model web site.

[http://lyra.oma.be/radiometric\\_model/radiometric\\_model.php](http://lyra.oma.be/radiometric_model/radiometric_model.php)



**Table 2:** Expected output signals (w/o uncertainties) between 110-240nm and purities in LYRA channels for minimum and maximum solar activity conditions.

Expected SIGNAL and Purity			at Solar Min	at Solar Max
<b>HEAD 1</b>	<b>Channel 1</b>	<b>Ly-<math>\alpha</math> (XN122)</b>	219.3pA [33.3%]	250.9pA [39.9%]
	<b>Channel 2</b>	<b>Herzberg</b>	11.23nA [83.1%]	11.25nA [83%]
	<b>Channel 3</b>	<b>Aluminium</b>		
	<b>Channel 4</b>	<b>Zirconium</b>		
<hr/>				
<b>HEAD 2</b>	<b>Channel 1</b>	<b>Ly-<math>\alpha</math> (XN122)</b>	162.61pA [17%]	175.87pA [21.5%]
	<b>Channel 2</b>	<b>Herzberg</b>	14.87nA [83.5%]	14.89nA [83.4%]
	<b>Channel 3</b>	<b>Aluminium</b>		
	<b>Channel 4</b>	<b>Zirconium</b>		
<hr/>				
<b>HEAD 3</b>	<b>Channel 1</b>	<b>Ly-<math>\alpha</math> (XN122+N)</b>	122.42pA [82.8%]	161.62pA [86%]
	<b>Channel 2</b>	<b>Herzberg</b>	11.04nA [83.1%]	11.05nA [83 %]
	<b>Channel 3</b>	<b>Aluminium</b>		
	<b>Channel 4</b>	<b>Zirconium</b>		

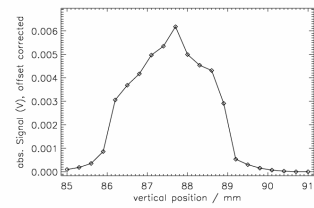
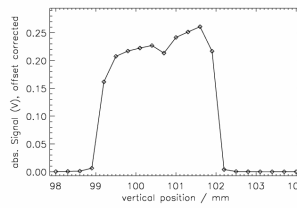
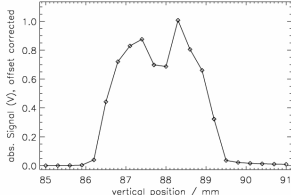
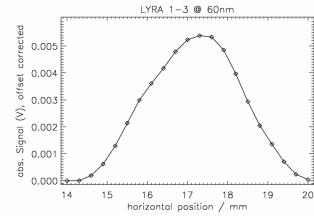
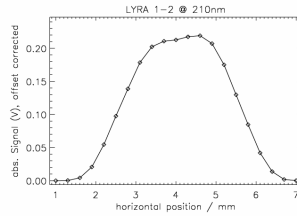
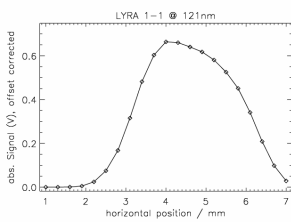
**Warning:** At Ly- $\alpha$ , we measure high signal and less purity. Note that the purity of Herzberg and AXUV channels should be taken with caution since not the entire visible spectrum is taken into account (measured data stop at 240nm, [we rather have an upper limit here](#)). Unfortunately we don't have the filters transmittance data in the near UV-Visible range and no MSM spare detectors for testing.



### 3 Homogeneity

Homogeneity was measured in two perpendicular directions at 121.6nm (for Ly- $\alpha$  channels), at 210nm (for Herzberg channels), and at 60nm for Al channels (1-3, 2-3 and 3-3) where “horizontal” means the short side of the LYRA instrument and “vertical” the long side. The offset voltages are subtracted.

#### 3.1 HEAD 1: Ch 1-1; 1-2; 1-3

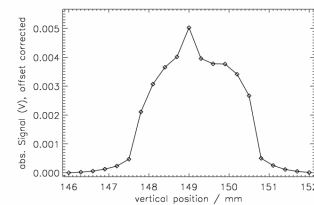
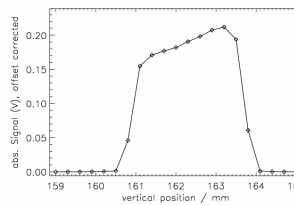
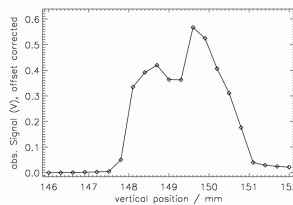
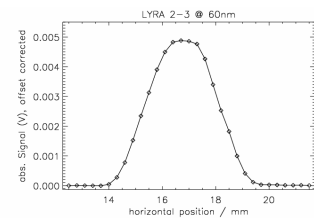
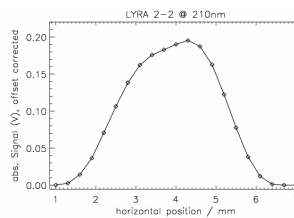
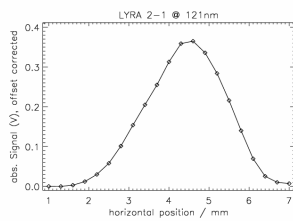


MSM12-Lyman- $\alpha$  (XN filter)

PIN10-Herzberg

MSM11-Aluminium

#### 3.2 HEAD 2: Ch 2-1; 2-2; 2-3



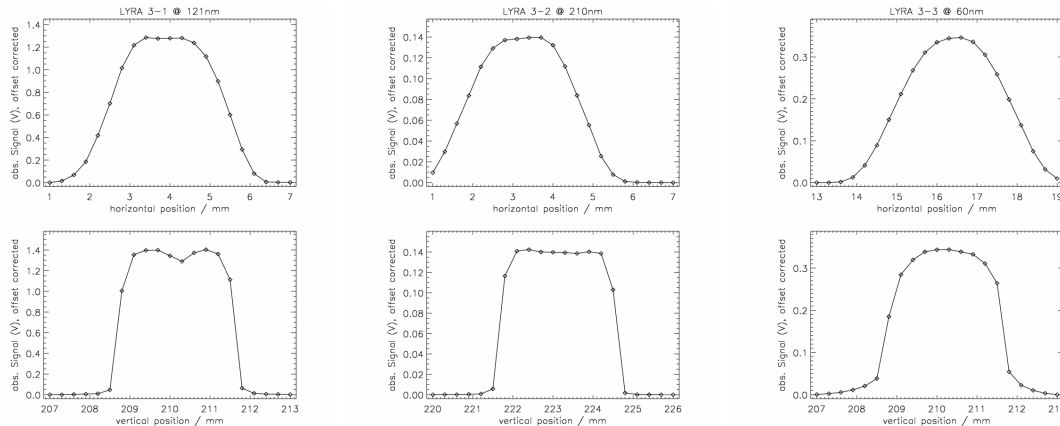
MSM21-Lyman- $\alpha$  (XN filter)

PIN11-Herzberg

MSM15-Aluminium



### 3.3 HEAD 3: Ch 3-1; 3-2; 3-3



AXUV#56-Lyman- $\alpha$  (XN+N filters)

PIN12-Herzberg

AXUV#59-Aluminium

Note that the impact of the full beam size (2mm horizontal x 1mm vertical) on the measured profile must be taken into account.

## 4 CONCLUSION

### Channels (1-1 and 2-1) at Ly- $\alpha$ :

Due to instability and dark current drift of the MSM channels, the uncertainty is very high (around 11% for MSM12 and 15% for MSM21). Channel 1-1 is not stable under photon flux and channel 2-1 looks better. Neither of them are uniform. According to our radiometric model the purity of these two channels is very low: 33% for Ch 1-1 (MSM12) and 17% for Ch 2-1 (MSM21), respectively, at Solar minimum condition.

### Channels (3-1) at Ly- $\alpha$ :

The silicon AXUV#56 diode looks slightly unstable after long photon flux exposure (at  $T=60^{\circ}\text{C}$ ). According to the new radiometric model, this channel gives a good expected signal but the actual purity is lower than noted here if taking into account the high solar spectrum contribution long wards of 240nm wavelength.

### Channels (2-1; 2-2 and 3-2) at 210nm:

All diamond PINs channels (Herzberg channels) seem to be stable at 210nm under photon flux with a good signal/dark current ratio and are reasonably homogenous over the active area.



## 5 ANNEXE

Using the hypothesis that the detector's response are correct, we deduced the Ly- $\alpha$  XN122 filter's transmittance from the different LYRA channels (i.e ch 1-1, 2-1 and 3-1). For the former one, the data were divided by the N122 filter transmittance (data from Acton R.).

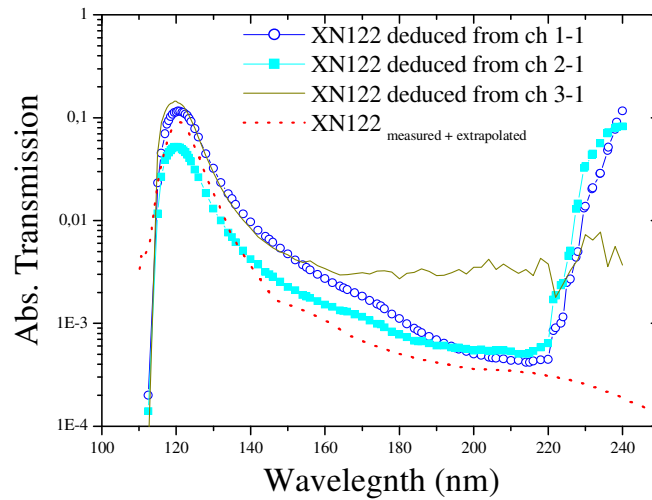


**Figure 7.** Absolute transmittance of the XN122 filter deduced from channel 1-1, 2-1 and 3-1 between 110nm and 240 nm. For comparison, the dotted line represents the model used in the LYRA radiometric model (Filter 122XN extrap.).

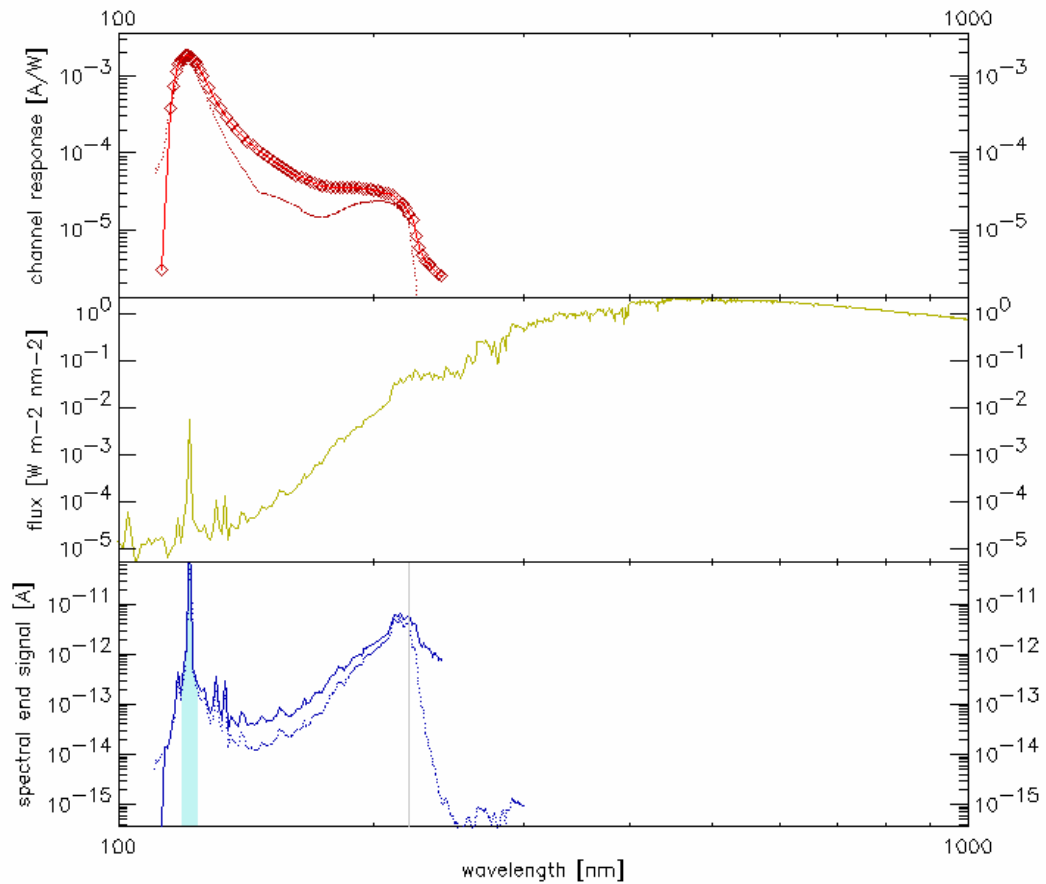
As seen in Fig.7, the data longwards 220nm should be taken with caution. One explanation might come from the impossibility to measure the high rejection (expected) at NI beamline.

**Table 3:** Expected output signals **between 110-220nm** and purities (width 2.5nm) in LYRA channels for minimum solar activity conditions.

Expected SIGNAL and Purity			at Solar Min	at Solar Min
			using Bessy-NI data	Updated Radiometric Model
<b>HEAD 1</b>	<b>Channel 1</b>	<b>Ly-<math>\alpha</math> (XN122)</b>	179.81pA [40.6%]	133.77 pA [42.4%]
<b>HEAD 2</b>	<b>Channel 1</b>	<b>Ly-<math>\alpha</math> (XN122)</b>	125.36pA [22%]	112.18 pA [43.8%]
<b>HEAD 3</b>	<b>Channel 1</b>	<b>Ly-<math>\alpha</math> (XN122+N)</b>	113.912 pA [89%]	80.21 pA [96%]



Assuming the 220nm cutoff, the following figures compare the measured response curves (square brackets) with those predicted from the RM (dotted curves round brackets). Data fit better with our updated radiometric model except the purity of channel 2-1 where the difference is almost 50%.



### Head 1 Channel 1

top panel: filter(s) + detector: Ly $\alpha$  122XN extrapolated + MSM12

middle panel: solar minimum spectrum

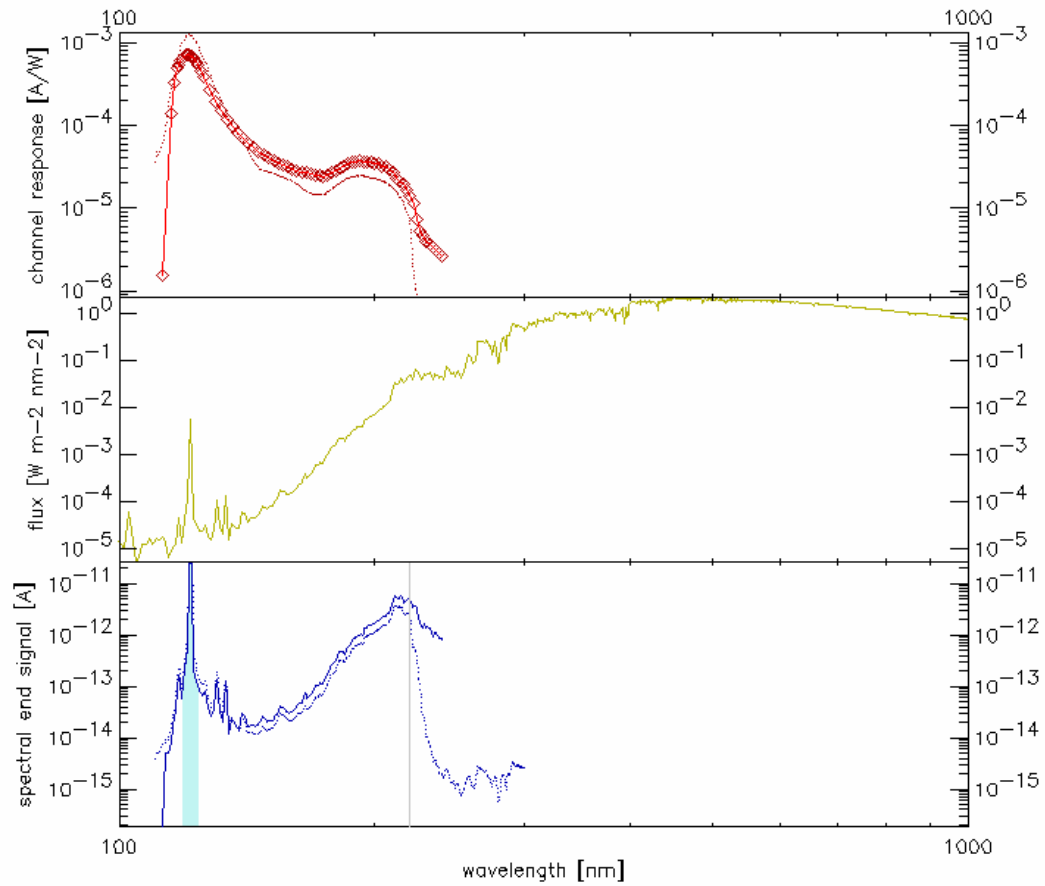
lower panel: total signal, integrated = 219.309 pA (133.767 pA) [179.807 pA]

purity in Ly $\alpha$  121.5: 33.3% (42.4%) [40.6%]

values in () and [] assume zero signal longwards of 220nm

dotted curves and () give results if individual filter and detector measurements are used





### Head 2 Channel 1

top panel: filter(s) + detector: Ly $\alpha$  122XN extrapolated + MSM21

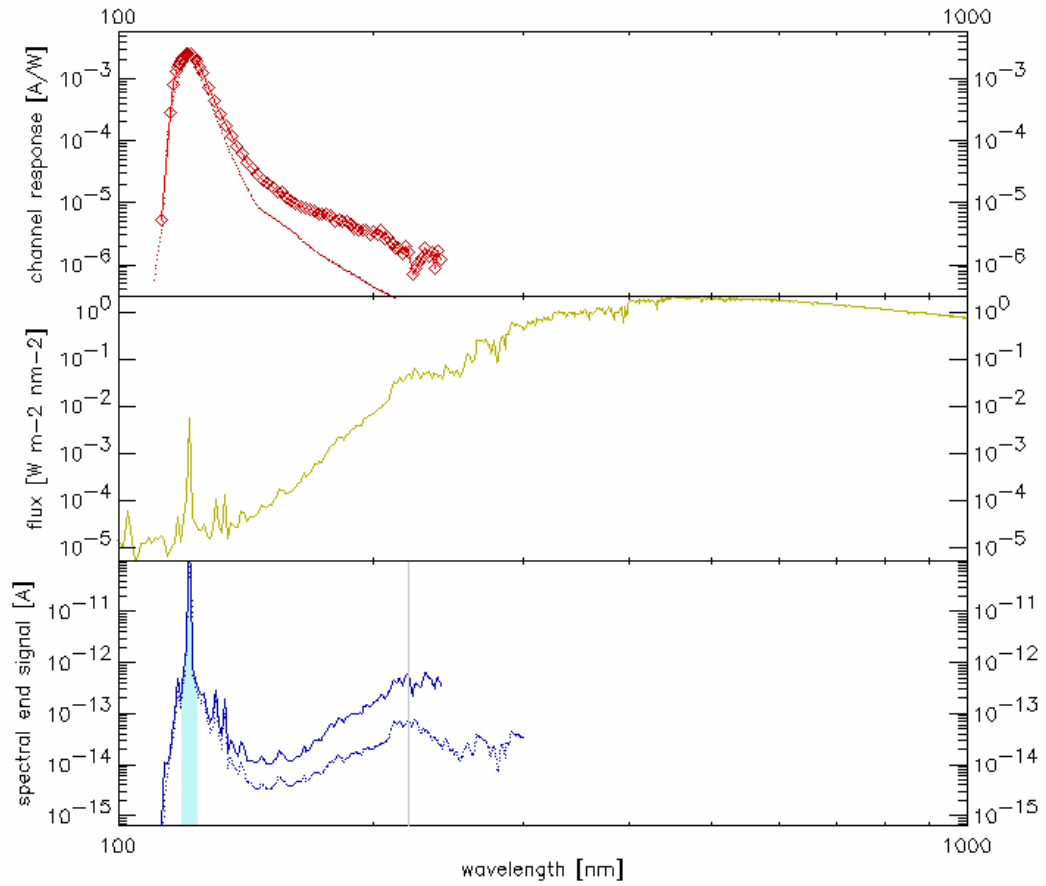
middle panel: solar minimum spectrum

lower panel: total signal, integrated = 162.610 pA (112.181 pA) [125.360 pA]

purity in Ly $\alpha$  121.5: 17.0% (43.8%) [22.0%]

values in () and [] assume zero signal longwards of 220nm

dotted curves and () give results if individual filter and detector measurements are used



### Head 3 Channel 1

top panel: filter(s) + detector: Ly $\alpha$  122XN extrapolated + Ly $\alpha$  122N + AXUV

middle panel: solar minimum spectrum

lower panel: total signal, integrated = 122.425 pA (80.212 pA) [113.912 pA]

purity in Ly $\alpha$  121.5: 82.8% (96.0%) [89.0%]

values in () and [] assume zero signal longwards of 220nm

dotted curves and () give results if individual filter and detector measurements are used